Click Here for Full Article

Physical and biological regulation of the soft tissue carbon pump

P. Parekh,[1] M. J. Follows,[2] S. Dutkiewicz,[2] and T. Ito[3]

Received 20 December 2005; revised 20 March 2006; accepted 4 April 2006; published 14 July 2006.

[1] We examine the relationship between aeolian iron deposition, ocean circulation, and atmospheric CO_2 in the context of a global ocean circulation and biogeochemistry model with a coupled atmospheric reservoir of CO_2. In common with previous models we find only a small reduction of atmospheric pCO_2 in response to an enhanced aeolian iron source consistent with Last Glacial Maximum conditions. We show this to be due to a combination of limiting factors including control of deep ocean iron concentrations by complexation to an organic ligand, regional compensation in changes to export production, and the maintenance of high preformed nutrient concentrations in deep water formation regions. We also demonstrate a significant sensitivity of atmospheric pCO_2 to changes in the residual mean overturning circulation of the Southern Ocean dominated by its regulation of the accumulation of biogenic carbon in the deep ocean. Although it is not enough to explain the full drawdown of pCO_2 to glacial levels, a reduction in overturning can lead to significant reduction in atmospheric pCO_2, providing mechanistic basis for the control by ''vertical mixing'' inferred from box models.

Citation: Parekh, P., M. J. Follows, S. Dutkiewicz, and T. Ito (2006), Physical and biological regulation of the soft tissue carbon pump, *Paleoceanography*, *21*, PA3001, doi:10.1029/2005PA001258.

1. Introduction

[2] Ice core records show that atmospheric pCO_2 was approximately 80–100 ppmv lower during the Last Glacial Maximum (LGM) than the preindustrial interglacial value of 280 ppmv [*Barnola et al.*, 1987; *Petit et al.*, 1999]. The cause of atmospheric pCO_2 variations between glacial and interglacial times are not well understood and there have been a number of oceanic mechanisms proposed [*Sigman and Boyle*, 2000]. Some of these mechanisms are linked to the physics of the ocean: enhanced sea ice coverage in the Southern Ocean to prevent outgassing of pCO_2 [*Stephens and Keeling*, 2000; *Keeling and Stephens*, 2001] or changes to stratification or mixing in the Southern Ocean [*Francois et al.*, 1997; *Toggweiler*, 1999; *Gildor and Tziperman*, 2001]. Other hypotheses focus on biogeochemical mechanisms, such as iron fertilization [*Martin*, 1990; *Kumar et al.*, 1995] and changes in the marine calcium carbonate budget [*Sigman et al.*, 1998]. These, and other hypotheses, are reviewed by *Sigman and Boyle* [2000]. In this manuscript we explore physical and biogeochemical mechanisms underlying some of the hypotheses in the context of a suite of sensitivity studies with a numerical model.

[3] One compelling biogeochemical mechanism, proposed by *Martin* [1990], was that an increase in the dust flux and supply of iron during the last LGM could have fertilized the remote Southern Ocean and increased the efficiency of the soft-tissue biological pump, thereby decreasing atmospheric carbon dioxide. This is consistent with evidence of an increase in the aeolian source of dust during glacial periods [*Petit et al.*, 1999]. In situ iron fertilization experiments have indeed demonstrated that primary productivity is limited by iron in high-nutrient, low-chlorophyll regions of the ocean [*Martin et al.*, 1994; *Coale et al.*, 1996; *Boyd et al.*, 2000; *Tsuda et al.*, 2003; *Boyd et al.*, 2004] and modest increases in export production have been observed following these experiments [*Buesseler et al.*, 2004; *Boyd et al.*, 2004]. Numerical models provide a framework in which to explore the implications on the global scale. Current limitations in the understanding of the biogeochemistry of iron in the ocean and the sparsity of ocean iron observations indicate that such models are still very speculative (including this one). Box models have suggested a wide range of responses to glacial levels of aeolian dust transport (up to 40 ppmv) [*Lefèvre and Watson*, 1999; *Watson et al.*, 2000], while in the current generation of three-dimensional models it drives only a small fraction of the observed change in pCO_2 (8–15 ppmv) [*Archer et al.*, 2000; *Bopp et al.*, 2003; *Parekh et al.*, 2006; this study]. Here we seek to understand what prevents a stronger response in these models.

[4] It has also been suggested that an increase in Southern Ocean stratification [*Francois et al.*, 1997] could lead to enhanced nutrient utilization, a more efficient biological pump, and a significant reduction of atmospheric pCO_2. In box model studies a reduction in Southern Ocean vertical mixing can have similar effect [*Toggweiler*, 1999; *Gildor and Tziperman*, 2001] though what dynamical processes the changes in vertical mixing coefficients represents is not quite clear. *Keeling and Visbeck* [2001] suggest that the relationship may be more complex because of the regulation of the residual mean overturning by stratification in the

[1]Climate and Environmental Physics, Physics Institute, University of Bern, Bern, Switzerland.
[2]Department of Earth, Atmosphere and Planetary Sciences, Massachusetts Institute of Technology, Cambridge, Massachusetts, USA.
[3]Joint Study for the Study of Atmosphere and Ocean, University of Washington, Seattle, Washington, USA.

Copyright 2006 by the American Geophysical Union.
0883-8305/06/2005PA001258$12.00

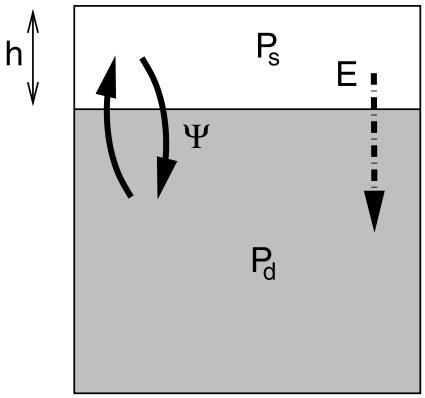

Figure 1. Two-layer schematic of the ocean phosphorus cycle. Here h (m) is the depth of the euphotic zone, and Ψ is the residual mean overturning rate (Sv). P_s is the surface phosphate concentration, and P_d is that in the deep ocean. E (mol P m^{-2} s^{-1}) is the rate of biological export of phosphorus, which is remineralized in the deep reservoir.

Southern Ocean. The residual mean flow, i.e., the net transport by Eulerian mean and eddy advection, is controlled by surface wind stress and buoyancy forcing [*Marshall*, 1997; *Karsten and Marshall*, 2002] and regulates the delivery of macronutrients and iron from the circumpolar deep waters to the surface [*Ito et al.*, 2005]. This is perhaps the dominant global pathway for the return of nutrients from the deep ocean to the surface. The residual mean flow also regulates the residence time of the upwelled waters in the surface circumpolar ocean and the transit time between upwelling and subduction during intermediate, or mode water, formation. Here we seek to clarify how the Southern Ocean residual mean overturning affects the local cycling of iron, phosphorus, carbon and, ultimately, atmospheric CO_2.

[5] In a suite of idealized sensitivity studies with a numerical ocean circulation and biogeochemistry model with a coupled atmospheric reservoir of carbon dioxide, we examine the response of the atmospheric pCO_2 to a broad range of variations in the aeolian dust source and residual overturning circulation. Here we extend the preliminary analysis of *Parekh et al.* [2006], which examined the sensitivity to dust flux only, in the broader context of climatic change including variations of ocean circulation. In section 2 we outline a simple, but qualitatively useful theoretical framework with which to relate "nutrient utilization," export production, and the residual mean circulation to atmospheric pCO_2. We then describe the ocean model (section 3) and discuss the implications of a series of sensitivity studies. We note that the model studies do not attempt to simulate in detail the state of the ocean at the LGM. Indeed we make some strong assumptions, such as assuming a closed ocean-atmosphere carbon system, which would prevent that. Rather we seek to understand some of the ocean's physical and biogeochemical controls on atmospheric carbon dioxide. We explore a variety of forcing scenarios, some of which might relate to colder, glacial climates, while others are more relevant to warmer climates than present day.

[6] Consistent with previous studies, atmospheric pCO_2 in this model has only a small response to an increased aeolian iron source. We show that this is due to a combination of physical and biogeochemical caps on the efficiency of the ocean's soft tissue pump. In contrast, we find a very strong response to a reduction in the aeolian iron source which may be relevant to periods of warmer climate than today's. Likewise we also demonstrate that atmospheric pCO_2 is very sensitive to changes in Southern Ocean residual mean overturning.

2. Simple Theoretical Framework: Nutrient Utilization

[7] We first present a highly idealized model which provides guidance when interpreting the complex, three-dimensional numerical model experiments. We note in advance that this simple framework is presented as an aid to qualitative interpretation of the general circulation model (GCM) results. Owing to the many simplifications and assumptions, the simple framework cannot be expected to accurately capture the quantitative aspects of the more complex model.

[8] Atmospheric pCO_2 is controlled not by the rate of export production alone, but by the efficiency of "nutrient utilization"; the fraction of total upwelled nutrients that is returned to depth in organic form [*Francois et al.*, 1997; *Sigman and Boyle*, 2000; *Ito and Follows*, 2005]. This can be illustrated simply in a two-box model representing the euphotic layer and deep ocean (Figure 1). In this framework, a prognostic equation may be written for the surface phosphate concentration, PO_{4s},

$$V_s \frac{dPO_{4s}}{dt} = -\Psi(PO_{4s} - PO_{4d}) - E \qquad (1)$$

where PO_{4d} is the phosphate concentration of the deep box, E (mol P s^{-1}) is the global export of phosphorus, and V_s (m^3) the volume of the surface ocean reservoir (i.e., euphotic zone). Ψ (10^6 m^3 s^{-1}) represents the exchange of surface and deep waters which we argue is dominated by the action of the residual mean overturning circulation. We define deep ocean phosphate as the sum of preformed (i.e., that brought into the interior by physical transport) and biogenic contributions (i.e., that which sinks as organic matter and remineralizes at depth): $PO_{4d} = PO_{4pre} + PO_{4bio}$. In this highly idealized framework, preformed phosphate is simply equivalent to the surface concentration: $PO_{4pre} = PO_{4s}$. If we assume steady state, the biological contribution of phosphate to the deep ocean, PO_{4bio}, is set by the competition between export production, E, and the upward transport of nutrients by ocean overturning, Ψ;

$$PO_{4bio} \sim \frac{E}{\Psi} \qquad (2)$$

[9] If biological transformations occur in fixed elemental ratios [*Redfield*, 1958],then the storage of carbon in the deep ocean directly attributable to the soft tissue pump is linearly related to PO_{4bio}. Thus an increase in PO_{4bio} would increase

the ocean's soft tissue pump, reducing atmospheric pCO_2 in a closed system. This suggests a simple relationship between aeolian iron source and pCO_2 when ocean circulation is fixed: Relieving iron fertilization increases export, enhances nutrient utilization and reduces atmospheric pCO_2. Changes in overturning have more complex implications since export, E is not independent of the circulation. However, if export were fixed, increasing overturning should lead to an increase in atmospheric pCO_2 because the residence time of deep waters is reduced and so too, the accumulation of remineralized organic carbon.

[10] This relationship between PO_{4bio} and pCO_2 can be developed more formally and quantitatively in terms of nutrient utilization [see *Ito and Follows*, 2005]. Here we simply note that equation (2) illustrates that it is the relative strength of export production and ocean circulation that is key to understanding the control of the soft tissue pump on atmospheric pCO_2. Here we explore the sensitivity to perturbations of both export and overturning in the context of a global circulation and biogeochemistry model.

3. Model Formulation

3.1. Physical Model

[11] We overlay coupled carbon, iron and phosphorus cycle models on the MIT ocean circulation model [*Marshall et al.*, 1997a, 1997b; *Adcroft et al.*, 1997] configured globally at coarse resolution (2.8×2.8 degrees, 15 vertical levels). The physical model is forced with a climatological annual cycle of surface wind stresses [*Trenberth et al.*, 1989], surface heat and freshwater fluxes [*Jiang et al.*, 1999] with additional relaxation toward climatological sea surface temperature and salinity [*Levitus and Boyer*, 1994; *Levitus et al.*, 1994]. In these coarse resolution studies, the effect of mesoscale eddy transfers is parameterized following *Gent and McWilliams* [1990]. Vertical turbulent mixing in the ocean is represented through a simple convective adjustment scheme. This configuration of the ocean model is similar to that used by *Dutkiewicz et al.* [2005] and *Parekh et al.* [2005].

3.2. Biogeochemical Model

[12] We model the coupled carbon, phosphorus and iron cycles using a simplified parameterization of export production in which biological uptake and regeneration are indexed to phosphorus. We carry six biogeochemical tracers in the model, phosphate (PO_4), dissolved organic phosphorus (DOP), dissolved inorganic carbon (DIC), alkalinity, oxygen (O_2) and dissolved iron (Fe_T). The tracers are transported by the modeled circulation and mixing processes.

[13] The biological consumption of phosphate is limited by the availability of light (I) and Fe or PO_4 and is parameterized as

$$B = \alpha \frac{I}{I + K_I} \min\left(\frac{\mathrm{PO_4}}{\mathrm{PO_4} + K_{\mathrm{PO_4}}}, \frac{\mathrm{Fe}}{\mathrm{Fe} + K_{Fe}}\right) \qquad (3)$$

following *McKinley et al.* [2004] and *Parekh et al.* [2005]. Here $\alpha = 0.17$ μM P month^{-1} and is the maximum consumption rate; the half-saturation constants are $K_I = 30$ W m^{-2}, $K_{PO4} = 0.5$ μM and $K_{Fe} = 0.12$ nM. A fraction, $\nu = 0.67$, of productivity, B, enters the DOP pool, which has an e-folding timescale for remineralization of 6 months [*Archer et al.*, 1997; *Yamanaka and Tajika*, 1997]. The remaining fraction is instantaneously exported as sinking particulate and is remineralized at depth according to the empirical relationship of *Martin et al.* [1987]. We assume that biological transformations of carbon and iron are linked to those of phosphorus by fixed elemental ratios ($R_{C:P}$, $R_{Fe:P}$). Here we use the term "export production" to refer to the component of net community production which becomes sinking organic particles, $(1 - \nu)$ B.

[14] The ocean carbon cycle model is coupled to a simple, well-mixed atmospheric reservoir of CO_2 [*Ito and Follows*, 2003]. Air-sea exchange of CO_2 is parameterized as a function of local wind speed following *Wanninkhof* [1992] and the equilibrium partitioning of dissolved inorganic carbon among the carbonate species is explicitly solved [*Follows et al.*, 2006].

[15] We explicitly represent the oceanic cycle of iron in the model following *Parekh et al.* [2004, 2005]. We impose an external aeolian source (Fe_{in}) as estimated with an atmospheric transport model [*Luo et al.*, 2003] and here assume a uniform solubility, $\alpha_{Fe} = 1\%$. Following *Parekh et al.* [2004], dissolved iron is partitioned into free, Fe′, and complexed, FeL, forms. A uniform concentration of total organic ligand, L_T, is imposed and can also partition into free and complexed forms. We assume rapid thermodynamic equilibration [*Witter et al.*, 2000], governed by the relation $K_{FeL} = [FeL]/[Fe'][L']$, where the conditional stability coefficient, $\log_{10}(K_{FeL}) = 11$, lies within the range estimated from laboratory and field studies. While the imposed total ligand concentration of 1 nM is higher than that assumed in some previous models (see discussion in section 4.1.2), it falls within the observed range [*Rue and Bruland*, 1995, 1997]. It also results in plausible modeled deepwater gradients of Fe_T and a ubiquitous presence of free ligand which is also consistent with observations [*Parekh et al.*, 2004, 2005]. In this model, Fe_T is available for biological consumption, but only Fe′ is susceptible to scavenging which is parameterized as a first-order process proportional to the free iron concentration [*Parekh et al.*, 2004] with a scavenging rate, k_{sc}, guided by those measured for thorium [*Bacon and Anderson*, 1982].

4. Model Results: Preindustrial Spin-up and Sensitivity Studies

[16] For the modern spin-up, we force the model with monthly aeolian dust deposition, estimated with an atmospheric transport model [*Luo et al.*, 2003] and assume that iron is 3.5% weight of the dust (Figure 2a). On the basis of sensitivity studies with a box model [*Parekh et al.*, 2004] and consistent with field and laboratory studies [*Jickells and Spokes*, 2002], we set the solubility of aeolian-derived Fe to 1%. It is likely that, in reality, the solubility varies significantly in space and time but there is, as yet, insufficient information to provide better constraint.

[17] After several thousand years of spin up with atmospheric pCO_2 held at 278 ppmv, the model closely

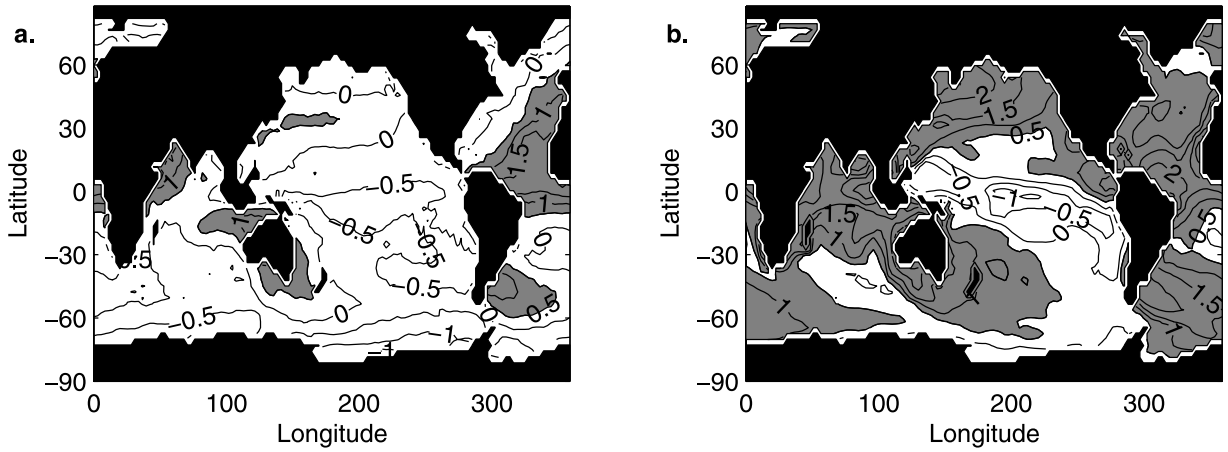

Figure 2. Modeled aeolian iron supply (mg Fe m^{-2} yr^{-1}) for the (a) modern climate [*Luo et al.*, 2003] and (b) Last Glacial Maximum (LGM) [*Mahowald et al.*, 1999]. Contours are in log scale. Shaded areas have log values greater than 0 (i.e., 1 n*M*). We assume 3.5 wt % of dust is iron and 1% is bioavailability.

approaches a steady, "preindustrial" state. The interplay of iron and phosphorus cycles leads to elevated surface PO_4 concentrations in the HNLC regions (Figure 3a), and the model reproduces the general character of the observed surface and deep water gradients of phosphate (Figures 3a and 3b). The distribution of DIC reflects a combination of solubility and biological controls (Figures 3c and 3d) with reduced surface concentrations and elevated levels at depth in the North Pacific. Though observations are as yet sparse, modeled surface iron concentrations are plausibly elevated in the surface waters of the Atlantic, Indian Ocean and the North Pacific (Figure 3e) which receive the strongest

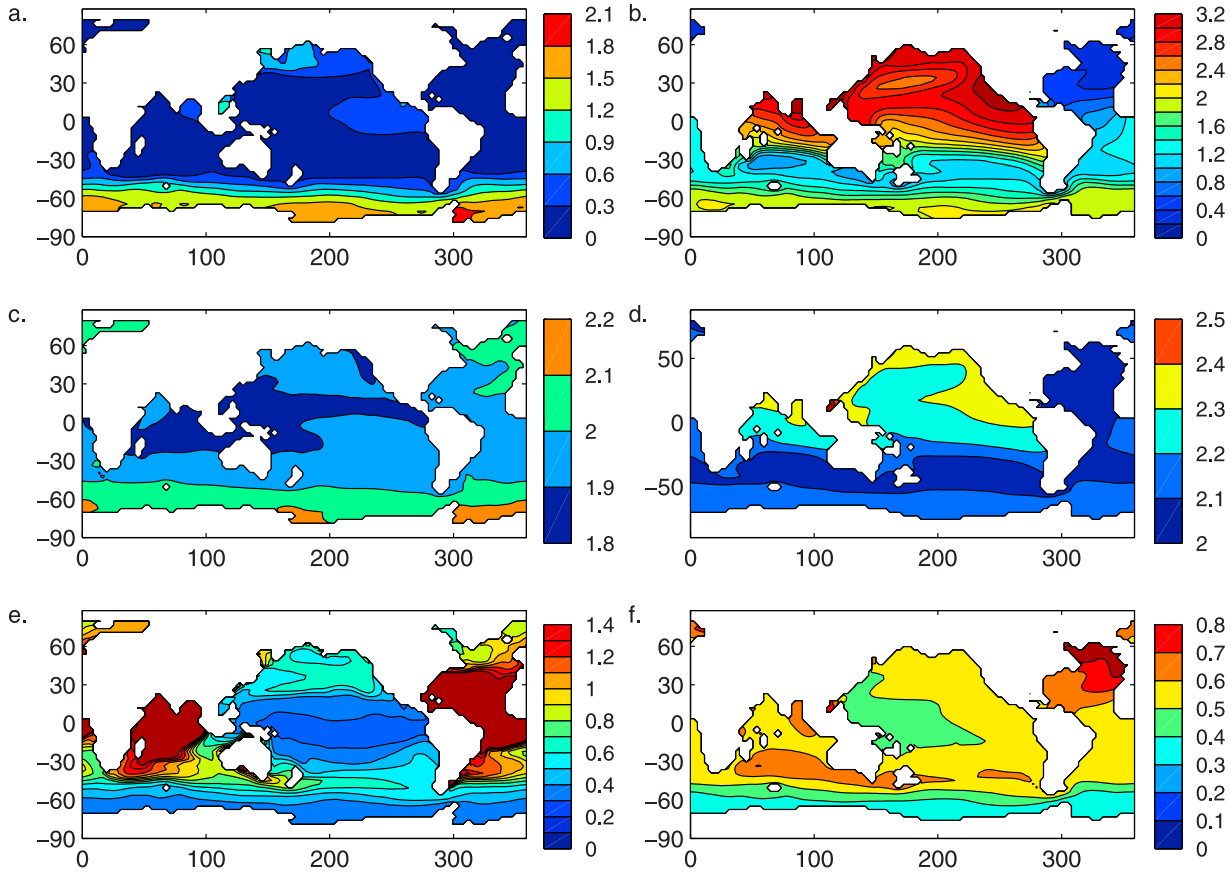

Figure 3. Model output from the control run: (a and b) PO_4 (μ*M*), (c and d) DIC (*M*), and (e and f) Fe_T (n*M*). (left) Surface concentrations. (right) Concentrations at 1000 m.

Table 1. Summary of Simulations

	Description	Dust	Ligand Concentration, nM	Wind	ΔpCO_2
EXP0	control	modern	1	normal	0
EXP1	LGM dust	LGM	1	normal	−8
EXP2	ligand	LGM	2	normal	−14
EXP3	50% decreased dust	50% modern	1	normal	+14
EXP4	90% decreased dust	10% modern	1	normal	+95
EXP5	no dust	no dust	1	normal	+181
EXP6	increased residual	LGM	1	50% increased S. Ocean westerlies	+25
EXP7	decreased residual	LGM	1	50% decreased S. Ocean westerlies	−31

aeolian supply. In the surface North Pacific, modeled [Fe_T] are somewhat higher than observed. At 1000 m (Figure 3f), the model suggests the highest concentrations are in the Northern Atlantic and Pacific waters and lowest [Fe_T] in the Southern Ocean, in broad agreement with the sparse observations [*Parekh et al.*, 2005].

[18] We perform a suite of sensitivity experiments, all initiated from the final state of the spin-up. In all sensitivity experiments the atmospheric reservoir of CO_2 is dynamic, regulated by global, net air-sea fluxes and the total burden of ocean-atmosphere carbon is conserved. Riverine sources and interactions with sediments are not represented. A control case (EXP0, Table 1), initialized by the spin-up, and with all forcings identical to the spin up, is integrated forward for a further 1000 years with dynamic atmospheric pCO_2. The seven sensitivity studies, in which biogeochemical or physical forcings are varied, are also initialized from the spun up state and integrated for an additional 1000 years to approach new, adjusted steady states (EXP1 to EXP7, Table 1). All biogeochemical changes in the sensitivity studies are referenced to the control case (EXP0).

4.1. Variations in Aeolian Iron Source

4.1.1. Increased Dust Source: LGM

[19] Data from ice cores [*Petit et al.*, 1999] and sediments [*Rea*, 1994] suggest that the aeolian iron supply in the Last Glacial period increased by up to 20 times locally in the Southern Ocean and 2–5 times globally, relative to present day. Here we apply LGM dust forcing estimated in a model of the linked terrestrial biosphere, dust source and atmospheric transport [*Mahowald et al.*, 1999] (Figure 2b). The ocean global aeolian iron source is 5.5 times higher than the modern aeolian forcing used in the preindustrial control, and 7.5 times higher in the Southern Ocean. Despite the significant increase in the aeolian iron source there is a only a small decrease in atmospheric pCO_2 relative to the control (EXP1 − EXP0) of only 8 ppmv after 1000 years, consistent with previously published models [*Archer and Johnson*, 2000; *Bopp et al.*, 2003; *Parekh et al.*, 2006]. A combination of mechanisms dictates this limited response:

4.1.1.1. Nonuniform Response of Export Production

[20] Equation (2) suggests a linear relationship between export production, E, and atmospheric pCO_2. However, despite a global, fivefold increase in aeolian iron supply (EXP1), globally integrated export production has increased by a mere 2% relative to the control (EXP0). There is not a uniform global increase in production (Figure 4), as noted by *Dutkiewicz et al.* [2005]. Indeed some regions of the model exhibit a decrease in export. Biological export is enhanced in the upwelling, HNLC regions which are iron-limited in modern (preindustrial) conditions. In contrast, export decreases in the subtropical gyres of the Pacific and throughout the Atlantic and Indian Ocean basins. The enhanced export in the HNLC regions reduces local surface phosphate concentrations and the lateral Ekman supply to the subtropical gyres [*Dutkiewicz et al.*, 2005; *Williams and Follows*, 1998]. Likewise, increased productivity in the Southern Ocean and Indo-Pacific upwelling regions reduces the lateral, upper ocean transport of macronutrients into the Atlantic basin. Since the Atlantic basin is generally iron replete, the reduction of available phosphate decreases basin-wide productivity [see *Dutkiewicz et al.*, 2005].

4.1.1.2. Complexation and Regulation of Deepwater Iron Concentration

[21] In addition, deep water iron chemistry and the strong control of the organic ligand on dissolved iron concentrations limit the effect of "iron fertilization" in the model. The major source of iron to the surface Southern Ocean is from upwelling water even in the LGM dust case (consistent with *Leféevre and Watson* [1999]). Consider the upwelling iron flux in the Southern Ocean, w_{res} Fe_T, where w_{res} is the residual mean upwelling velocity and Fe_T the total dissolved iron concentration. Since free iron, Fe', is rapidly scavenged, the deep ocean iron concentration cannot significantly exceed the total ligand concentration, L_T, except in very strong source regions. As the aeolian source increases, the upwelling supply asymptotes toward w_{res} L_T. As suggested by *Leféevre and Watson* [1999], the response of biological productivity in Southern Ocean is most sensitive to the iron supply in the northern basins through the deep water source. However, owing to the explicit parameterization of the control of deep ocean iron concentration by complexation, even the enhanced northern iron supply has a limited effect. (See also discussion of the sensitivity to ligand concentration; section 4.1.2.)

4.1.1.3. Physical Controls on High-Latitude Productivity and Preformed Nutrients

[22] Even in iron replete conditions in the modeled Southern Ocean, there is not a complete draw down of macronutrients. Why is this the case? At high latitudes where there is strong seasonality, significant ice cover and relatively deep summer mixed layers, light can be the dominant limiting factor for productivity [*Mitchell et al.*, 1991; *Popova et al.*, 2000; *van Oijen et al.*, 2004], reducing the sensitivity to iron supply. In particular the strong winter mixing and spring restratification in the restricted regions of deep water formation selects for high preformed nutrient concentrations in the deep waters [*Ito and Follows*, 2005]

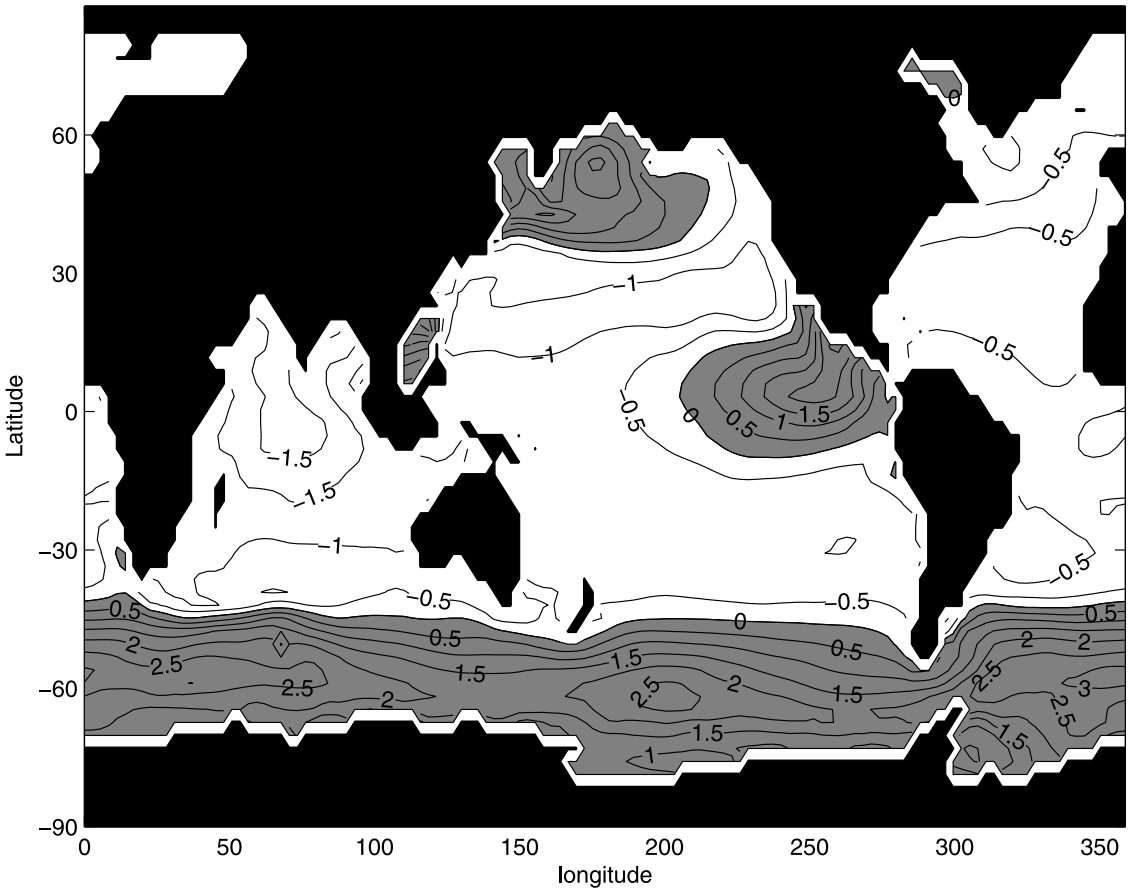

Figure 4. Difference in modeled export production between the LGM and modern (EXP1 − EXP0). Regions where export production increased are shaded. Units are in g C m^{-2} yr^{-1}.

even in iron replete conditions. Thus over wide areas of the high-latitude North Pacific and Southern Ocean, productivity and macronutrient utilization are ultimately limited by light and mixing dynamics. These factors conspire to cap global ocean export production and the response of the soft-tissue pump to increased aeolian iron supply.

4.1.2. Sensitivity to Ligand Concentration

[23] The complexing ligand plays a key role in the iron cycle and, in our model, regulates the sensitivity of the biological pumps and pCO_2 to the atmospheric iron source. Yet relatively little is known about the distribution of ligands and their sources and sinks in the ocean. Here, as did *Archer and Johnson* [2000], we impose a global uniform ligand concentration consistent with the few available observations [*Rue and Bruland*, 1995, 1997] and guided by sensitivity studies with a box model [*Parekh et al.*, 2004]. It has been conjectured that the ligand concentration may vary in response to changes in biological productivity. During the Iron-Ex II study, in the equatorial Pacific, ligand concentration increased with the addition of iron [*Rue and Bruland*, 1997].

[24] We have not applied such a parameter as this relationship is still not well understood. However, we do investigate what the consequences of a change in the imposed ligand concentration has on pCO_2. In a further sensitivity study (EXP2), we apply LGM aeolian dust forcing and also double the imposed total ligand concentration, $[L_T]$ = 2 n*M*. The simultaneous increase in ligand concentration and aeolian source almost doubles (14 ppmv) the response of atmospheric carbon dioxide relative to the LGM case (EXP1) alone. However this response is still small relative to observed glacial/interglacial changes in pCO_2.

[25] We stress that this experiment is simply used to illustrate how sensitive the system is to possible variations in ligand concentration but there is much to understand in that regard. The nature and role of the organic ligand(s) remains a key and open question in our understanding of the oceanic iron cycle with significant implication for the regulation of atmospheric CO_2 by the aoelian iron source.

4.1.3. Decreased Aeolian Iron Source

[26] Much of the focus on the role of iron has centered around fertilization of the HNLC regions in a windier, drier and dustier glacial climate, and how this might draw down atmospheric pCO_2. However, recent models, including this one, suggest only a small effect from iron fertilization alone. In contrast there has been little consideration of climates in which there may be a reduced iron delivery to the oceans. There have been periods in earth history with significantly warmer climates than today's; for example the Late Permian or the Late Paleocene. Such warmer climates are likely to be characterized by a more humid atmosphere because of the

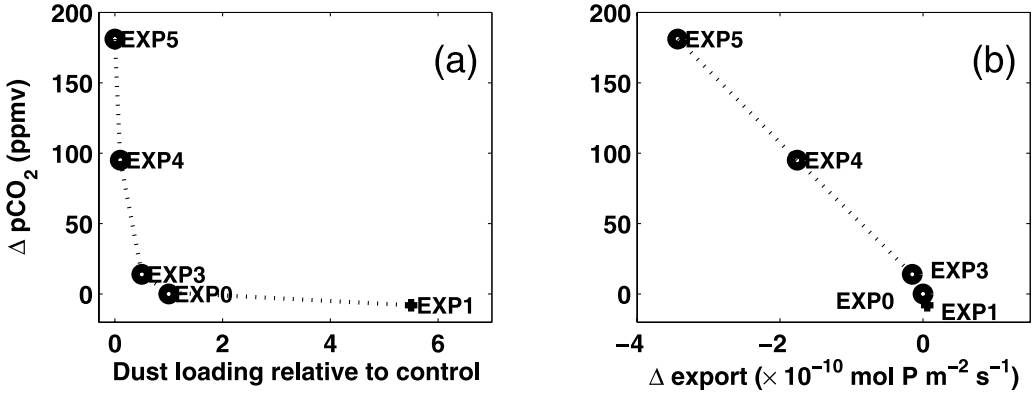

Figure 5. Sensitivity of pCO_2 to changes in (a) dust flux and (b) export production ($\times 10^{-10}$ mol P m^{-2} s^{-1}), relative to control (EXPO) after 1000 years. EXP1 (plus sign) uses LGM dust which is not an exact multiple of modern dust. EXP5 is not yet at steady state after 1000 years.

increase in saturation water vapor concentration and a more vigorous hydrologic cycle than today [*Farrell*, 1990]. Furthermore, warm climate conditions are associated with weaker meridional atmospheric temperature gradients, a weaker jet stream and, perhaps, generally less windy conditions [*Farrell*, 1990]. Such circumstances could conspire to reduce the continental sources of dust and its transport to the remote oceans [*Hovan and Rea*, 1992; *Rea et al.*, 1990; *Rea*, 1994]. How might a significant reduction in the aeolian iron source affect ocean productivity and atmospheric CO_2?

[27] In a previously published study [*Parekh et al.*, 2006], we show that pCO_2 is significantly more sensitive to decreasing dust flux relative to an increase in dust flux. We reduced the amplitude of the modern dust deposition pattern [*Luo et al.*, 2003] globally and examined the response in atmospheric pCO_2 after one thousand years (i.e., approaching a new steady state). Decreasing aeolian iron flux 50% (EXP3) results in a 14 ppmv increase in pCO_2, while a decrease of 90% (EXP4) results in a 94 ppmv increase [*Parekh et al.*, 2006] (Figure 5a). In the LGM scenario, we increased dust flux globally by a factor of 5.5 and our model only predicted a decrease in pCO_2 of 8 ppmv. In strong contrast, decreasing dust flux by a factor of 2 (EXP3) results in almost double the change in the opposite direction.

[28] We also perform a simulation in which we completely cut off dust supply (EXP5). After 1000 years, the model is still adjusting significantly, but pCO_2 has increased by 181 ppmv (Figure 5a). As the aeolian iron source is reduced, a larger area of the ocean experiences iron stress, resulting in decreased export production (Figure 5b). According to equation (2), since circulation (Ψ) is held fixed, a decrease in export (E) results in a decrease in PO_{4bio}, decreasing the ocean's soft tissue pump and increasing atmospheric pCO_2. Including sedimentary and riverine sources of iron may temper this response. In the next section we explore the effect circulation has on atmospheric pCO_2 concentrations.

4.2. Sensitivity to Residual Mean Overturning Circulation

[29] The consensus of recent GCM studies [*Archer et al.*, 2000; *Bopp et al.*, 2003; *Parekh et al.*, 2006; this study] is that increased dust fluxes alone can only explain a fraction of the glacial draw down in atmospheric pCO_2. Other studies, using box models, have suggested that a reduction in "vertical mixing" in the Southern Ocean can have a significant effect in drawing down atmospheric pCO_2 [*Toggweiler*, 1999; *Gildor and Tziperman*, 2001] (and review of *Sigman and Boyle* [2000]). What are the dynamics that are represented by this change in "vertical mixing" in such low-resolution models? *Keeling and Visbeck* [2001] highlighted the possible role of changes to the residual mean overturning circulation of the Southern Ocean. The residual mean flow, the net transport by Eulerian mean and eddy advection is intimately tied to the stratification and patterns of surface physical forcing [e.g., *Marshall*, 1997]. In the Southern Ocean it regulates the upwelling and delivery of macronutrients and iron from the circumpolar deep waters to the surface; perhaps the dominant pathway for the return of deep nutrients to the surface ocean. The residual mean flow also controls the residence time of the upwelled waters in the surface circumpolar ocean as they transit to regions of deep, intermediate, or mode water formation. How do changes in Southern Ocean residual mean overturning affect the local cycling of iron, phosphorus and carbon, and ultimately atmospheric CO_2?

[30] We address this question with a further suite of sensitivity experiments in which the residual flow is conveniently modulated by varying the wind stress field (though we might equally have produced a similar effect by controlling the air-sea buoyancy fluxes). Since we are particularly keen to explore the role of changes in the Southern Ocean, which plays a strong role in regulating the ocean's biological pump, we vary the wind stress field only in the Southern Hemisphere. Since the air-sea heat and freshwater fluxes in the model include a restoring component and we maintain the climatological "target" fields, the air-sea buoyancy flux adjusts such that the residual flow varies. (Note that if the air-sea buoyancy flux were not able to adjust there could be no change in the residual mean flow [*Walin*, 1982; *Marshall*, 1997].)

[31] In one case we double the intensity of the westerly wind stress in the Southern Ocean (EXP6) resulting in an enhanced residual mean flow; the "strong overturning"

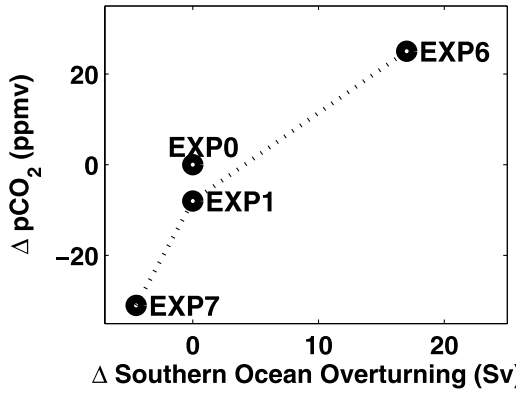

Figure 6. Sensitivity of atmospheric pCO_2 to changes in residual overturning relative to control run (EXP0). Perturbation runs were forced with LGM dust flux. Residual circulation was modulated by changing the Southern Ocean westerlies. Since EXP6 and EXP7 are run with LGM dust, we also include the LGM run with normal winds (EXP1) for comparison.

case. The maximum overturning at south of 40°S is 22 Sv; stronger than the 5 Sv of the control (EXP0). We also decrease the intensity of Southern Hemisphere westerlies by 50% leading to a "weak overturning" (EXP7) of about 1 Sv. In both experiments we spin the model up toward a new equilibrium state leading to new circulation patterns and an adjustment of the biological carbon pumps. In these cases we also apply LGM dust forcing in order to examine the combined effect of changes to circulation and the aeolian iron supply.

[32] We note that though the changes to wind stress are limited to the Southern Hemisphere and we are focusing on the Southern Hemisphere response because of the strong local control on the biological pump, there is also a clear response in the overturning circulation of the Northern basins, dominated by North Atlantic deep water formation [see *Toggweiler and Samuels*, 1998]. This is altered from 18 Sv in the control case (EXP0) to 24 Sv (EXP6) and 15 Sv (EXP7) in the strong and weak overturning cases, respectively. There are also associated changes in the ACC, Gulf Stream and Indonesian throughflow transports.

[33] Referencing to the LGM dust case with "modern" circulation (EXP1) there is a 33 ppmv increase in pCO_2 due entirely to the increased overturning rate (EXP6) and a 23 ppmv decrease when the overturning is reduced (EXP7). Referenced to the control run (EXPO), there is a 25 ppmv increase when overturning is increased (EXP6) and 31 ppmv decrease when overturning is decreased (EXP7) (Figure 6). Hence the residual mean circulation can exert a significant control on atmospheric pCO_2. Compare the difference of 8 ppmv between LGM dust forcing (EXP1) and control (EXP0) where the circulation is fixed. The changes in wind stress forcing lead to a modification of the residual mean overturning circulation, which affects not only the biological pumps of carbon but also the solubility pump because of changes in the physical structure of the ocean gyres and ventilated thermocline [*Ito and Follows*, 2003].

4.2.1. Soft-Tissue Pump

[34] As discussed in section 2, the efficiency of the soft tissue pump can be considered in terms of nutrient utilization which may be measured by the ratio of export production and overturning illustrated in the relationship of equation (2). However, export and overturning are not independent. Increasing the Southern Ocean residual overturning enhances the rate with which nutrients, both phosphate and iron, are brought up into the euphotic zone, driving an increase in export production in the region (Figure 7a). The opposite response occurs when the residual overturning is reduced (Figure 7b). The Atlantic basin is generally iron replete and macronutrient limited and its macronutrient supply is modulated by the northward, surface residual flow into the basin [*Dutkiewicz et al.*, 2005] and to the regions of intermediate and mode water formation [*Sarmiento et al.*, 2004]. With a stronger overturning

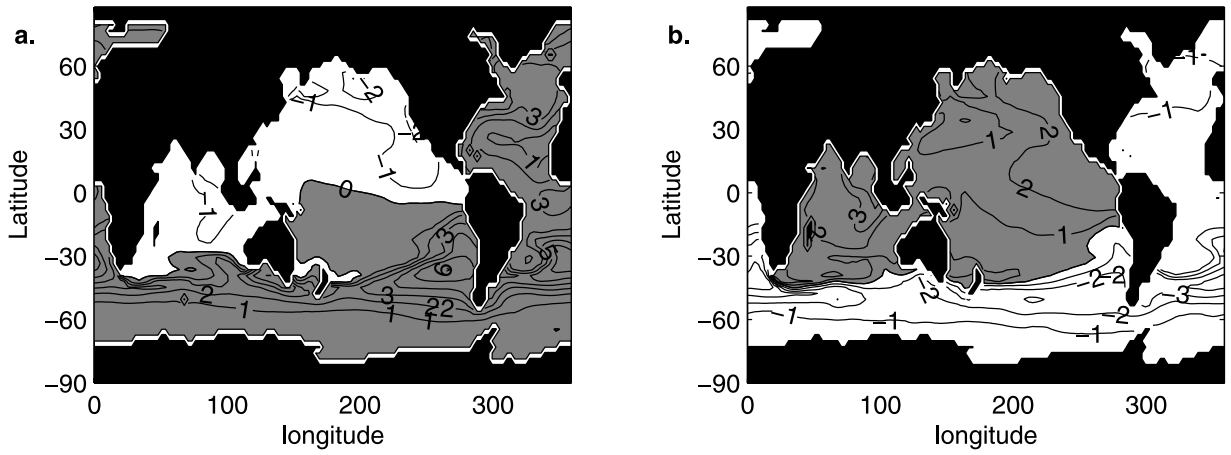

Figure 7. Difference in biological export in the top layer of the model (g C m^{-2} yr^{-1}) between (a) high-residual and LGM cases (EXP6 − EXP1) and (b) low-residual and LGM cases (EXP7 − EXP1). Shading indicates regions where biological export increased relative to LGM case (EXP1).

the surface-oriented lateral transfer of phosphate into the Atlantic is increased, enhancing basin wide productivity (Figure 7a). In contrast the Indo-Pacific basin is fed by inflow of bottom waters and does not benefit from the increased upper ocean overturning. The enhanced supply and net increase of macronutrients in the Atlantic basin thus occurs at the expense of the Indo-Pacific (seen simply in terms of a global conservation constraint) and these basins experience a decrease in productivity when the upper ocean overturning is increased. In contrast, the sluggish circulation of EXP7 (Figure 7b) reduces the vertical supply of phosphate and iron to the Southern Ocean euphotic zone, decreases the lateral transfer to the Atlantic basin, resulting in an accumulation of nutrients in the Pacific.

[35] Curiously, but owing to to the complex interactions of circulation and productivity, global export actually increases in both the stronger (EXP6, 14%) and weaker (EXP7, 5%) overturning cases, relative to the reference LGM run (EXP1). Hence, according to the simple view of equation (2), export changes so as to reduce pCO_2 with fixed Ψ. However, regional compensation in changes to export (Figure 7) leads to only moderate global change [*Dutkiewicz et al.*, 2005) and, from equation (2), it is clear that the dominant control on the soft-tissue pump is the direct effect of changing overturning in circulation which modulates the residence time of deep waters and hence their potential to accumulate biogenic carbon. Modulation of the soft tissue pump, dominated by the effect of changing deep ocean residence time, is consistent with the response of pCO_2 to changes in the modeled overturning.

4.2.2. Solubility Pump

[36] While the changes in pCO_2 are generally consistent with the modulation of the soft tissue pump there is another potentially significant mechanism at play. Since we also modify the circulation and hydrography of the ocean model, there is also some change to the (abiotic) solubility pump. To what extent do these affect pCO_2? We have used changes in wind stress forcing to manipulate the residual mean overturning circulation. Simple scalings and idealized numerical models indicate that an increase in wind stress forcing will reduce the ocean storage of carbon by the (abiotic) solubility pump [*Ito and Follows*, 2003]. As the wind stress increases, the boundary currents become swifter and the waters ventilating the subtropical thermocline are more undersaturated. In addition, the reservoir of warm thermocline waters, with low-saturation DIC, increases. Both effects drive carbon into the atmosphere as wind stress forcing increases, in accord with the response of the present model. The idealized models of *Ito and Follows* [2003] suggest that doubling the amplitude of wind stress forcing over one hemisphere could drive an increase of atmospheric pCO_2 of 5 to 10 ppmv, dependent upon the rate of diapycnal mixing. Hence we can explain the sensitivity of modeled pCO_2 to the modified circulation as a combination of changes to solubility and biological pumps.

5. Summary and Discussion

[37] We have examined the sensitivity of atmospheric pCO_2 in a global circulation and biogeochemistry model to changes in physical and biogeochemical boundary conditions including the strength of the aeolian iron source and the vigor of the residual mean overturning circulation in the Southern Ocean. While we do not attempt to simulate the conditions at the LGM, these model explorations enable us to comment on the possible role of several mechanisms which may regulate atmospheric CO_2 in that period and other, very different, climatic states. We point out that the numerical models presented here represent a set of idealized sensitivity studies which hopefully provide insight, but do not attempt to comprehensively simulate glacial-interglacial changes. We have focused on exploring select mechanisms and by necessity make some strong assumptions. For example, we only crudely represent organic ligand(s) which are not yet well understood [*Wells et al.*, 1995; *Macrellis et al.*, 2001] and recent work also shows that a significant fraction of ''dissolved'' iron is in colloidal form [*Wu et al.*, 2001], yet too little is known for us to incorporate this aspect at all. Likewise, the residual mean overturning of the model includes a parameterization of the effect of eddies since we cannot perform such a suite of sensitivity studies at mesoscale resolution on the global scale. With these cautions in mind, however, we believe that these numerical models provide some useful insights.

[38] In common with other recent numerical models, the response of atmospheric carbon dioxide to an increased aeolian supply of iron to the ocean, representative of that during the LGM, is too weak to explain the observed change in pCO_2 alone. In this model a 5.5-fold global increase in aeolian iron supply results in an 8 ppmv draw down of pCO_2 [cf. *Archer et al.*, 2000; *Bopp et al.*, 2003]. There are three mechanisms which lead to this limited response: First, the primary source of iron to the remote surface Southern Ocean of the model is due to upwelling. Thus, even with LGM aeolian dust transport, the upwelling iron concentration is limited by the fixed concentration of organic ligand. Secondly, regional compensation in response to an enhanced iron source means that changes to global export production are only modest. Finally, the nature of deep water formation in the model selects for high preformed nutrient concentrations and ultimately restricts the efficiency of the biological pump.

[39] However, we find a very asymmetrical response to changes in the dust source with a strong sensitivity to decreasing aeolian iron supply. We find that decreasing the aeolian source leads to a steady decline of dissolved iron concentrations, a weakened biological pump and higher atmospheric carbon dioxide concentrations. There is a strong, and continuing response as the dust source is reduced until there is a dead ocean.

[40] Could the ocean's carbon pumps have played a role in reducing atmospheric pCO_2 in glacial periods? In a further set of sensitivity studies we show that there is also considerable sensitivity to the vigor of Southern Ocean residual mean overturning. Enhanced overturning results in increased atmospheric pCO_2 and vice versa, dominated by the effect of changing the deep ocean residence time and accumulation of biogenic carbon. The model suggests a sensitivity of atmospheric pCO_2 of about 3 ppmv per Sverdrup change in Southern Ocean residual overturning

(slope of Figure 6). Hence changes in wind stress and buoyancy forcing, which control the residual mean flow, may be a significant regulatory mechanism and provide a plausible physical framework for variations in ''vertical mixing'' invoked by low-resolution box models.

[41] Using a three-dimensional global ocean circulation and biogeochemistry model we have demonstrated that pCO_2 is indeed sensitive to changes in dust flux and circulation. Owing to many uncertainties we have not tried to ''recreate'' the LGM, rather we have isolated biogeochemical and physical mechanisms that place controls on pCO_2. In common with previous box model studies, we identify a significant sensitivity of the ocean-atmosphere iron and carbon cycles to changes in climate and ocean circulation. In box models this has been parameterized as an unidentified, generic vertical mixing process. Here we show that the agent of this sensitivity could be the residual mean flow (the net effect of the mean flow and eddy transfers) in the high-latitude Southern Ocean. Our study also highlights the importance of the organic ligand in regulating the availability of iron and productivity at high southern latitudes. Sensitivity of atmospheric CO_2 to the external source of iron is strongly dependent upon the deep ocean ligand concentration. It is critical that the nature and cycling of chelators of iron in the ocean are better understood if we are to improve our understanding of these sensitivities.

[42] **Acknowledgments.** M.J.F. and P.P. are grateful for funding from NSF (OCE-336839). We thank David Archer and an anonymous reviewer for their constructive comments.

References

Adcroft, A., C. Hill, and J. Marshall (1997), Representation of topography by shaved cells in a height coordinate ocean model, *Mon. Weather Rev.*, *125*, 2293–2315.

Archer, D., and K. Johnson (2000), A model of the iron cycle in the ocean, *Global Biogeochem. Cycles*, *14*, 269–279.

Archer, D., E. Peltzer, and D. Kirchman (1997), A timescale for dissolved organic carbon production in equatorial Pacific surface waters, *Global Biogeochem. Cycles*, *11*, 435–452.

Archer, D., A. Winguth, D. Lea, and N. Mahowald (2000), What caused the glacial/interglacial atmospheric pCO_2 cycles?, *Rev. Geophys.*, *38*, 159–189.

Bacon, M., and R. Anderson (1982), Distribution of thorium isotopes between dissolved and particulate forms in the deep sea, *J. Geophys. Res.*, *87*, 2045–2056.

Barnola, J., D. Raynaud, Y. Korotkevich, and C. Lorius (1987), Vostok ice core provides 160,000–year record of atmospheric CO_2, *Nature*, *329*, 408–414.

Bopp, L., K. Kohfeld, C. L. Quéré, and O. Aumont (2003), Dust impact on marine biota and atmospheric CO_2 during glacial periods, *Paleoceanography*, *18*(2), 1046, doi:10.1029/2002PA000810.

Boyd, P., et al. (2000), A mesoscale phytoplankton bloom in the polar Southern Ocean stimulated by iron fertilization, *Nature*, *407*, 695–702.

Boyd, P., et al. (2004), The decline and fate of an iron-induced subarctic phytoplankton bloom, *Nature*, *428*, 549–553.

Buesseler, K., J. Andrews, S. Pike, and M. Charette (2004), The effects of iron fertilization on carbon sequestration in the Southern Ocean, *Science*, *304*, 414–417.

Coale, K., et al. (1996), A massive phytoplankton bloom induced by an ecosystem-scale iron fertilization experiment in the equatorial Pacific Ocean, *Nature*, *383*, 495–501.

Dutkiewicz, S., M. Follows, and P. Parekh (2005), Interactions of the iron and phosphorus cycles: A three-dimensional model study, *Global Biogeochem. Cycles*, *19*, GB1021, doi:10.1029/2004GB002342.

Farrell, B. (1990), Small error dynamics and the predictability of atmospheric flows, *J. Atmos. Sci.*, *47*, 2409–2416.

Follows, M., T. Ito, and S. Dutkiewicz (2006), On the solution of carbonate chemistry system in ocean biogeochemistry models, *Ocean Modell.*, *12*, 290–301.

Francois, R., M. Altabet, E. Yu, D. Sigman, M. Bacon, M. Frank, G. Bohrmann, G. Bareille, and L. Labeyrie (1997), Contribution of Southern Ocean surface-water stratification to low atmospheric CO_2 concentrations during the last glacial period, *Nature*, *389*, 929–935.

Gent, P., and J. McWilliams (1990), Isopycnal mixing in ocean circulation models, *J. Phys. Oceanogr.*, *22*, 625–651.

Gildor, H., and E. Tziperman (2001), Physical mechanisms behind biogeochemical glacial-interglacial CO_2 variations, *Geophys. Res. Lett.*, *28*, 2421–2424.

Hovan, S., and D. Rea (1992), Paleocene Eocene boundary changes in atmospheric and oceanic circulation—A Southern-Hemisphere record, *Geology*, *20*, 15–18.

Ito, T., and M. Follows (2003), Upper ocean control on the solubility pump of CO_2, *J. Mar. Res.*, *61*, 461–489.

Ito, T., and M. Follows (2005), Preformed phosphate, soft tissue pump and atmospheric CO_2, *J. Mar. Res.*, *63*, doi:10.1357/0022240054663231.

Ito, T., P. Parekh, S. Dutkiewicz, and M. Follows (2005), The Antarctic Circumpolar Productivity Belt, *Geophys. Res. Lett.*, *32*, L13604, doi:10.1029/2005GL023021.

Jiang, S., P. Stone, and P. Malanotte-Rizzoli (1999), An assessment of the geophysical fluid dynamics laboratory ocean model with coarse resolution: Annual-mean climatology, *J. Geophys. Res.*, *104*, 25,623–25,645.

Jickells, T. D., and L. Spokes (2002), Atmospheric iron inputs to the oceans, in *The Biogeochemistry of Iron in Seawater*, 1st ed., edited by D. R. Turner and K. A. Hunter, pp. 85–121, John Wiley, Hoboken, N. J.

Karsten, R., and J. Marshall (2002), Constructing the residual circulation of the ACC from observations, *J. Phys. Oceanogr.*, *32*, 3315–3327.

Keeling, R., and B. Stephens (2001), Antarctic sea ice and the control of Pleistocene climate instability, *Paleoceanography*, *16*, 112–131.

Keeling, R., and M. Visbeck (2001), Paleoceanography—Antarctic stratification and glacial CO_2, *Nature*, *412*, 605–606.

Kumar, N., R. Anderson, R. Mortlock, P. Froelich, P. Kubik, B. Dittrich-Hannen, and M. Suter (1995), Increased biological productivity and export production in the glacial Southern Ocean, *Nature*, *378*, 675–680.

Lefévre, N., and A. J. Watson (1999), Modeling the geochemical cycle of iron in the oceans and its impact on atmospheric CO_2 concentrations, *Global Biogeochem. Cycles*, *13*, 727–736.

Levitus, S., and T. Boyer (1994), *World Ocean Atlas 1994*, vol. 4, *Temperature, NOAA Atlas NESDIS*, vol. 4, 129 pp., NOAA, Silver Spring, Md.

Levitus, S., R. Burgett, and T. Boyer (1994), *World Ocean Atlas 1994*, vol. 3, *Salinity, NOAA Atlas NESDIS*, vol. 3, 111 pp., NOAA, Silver Spring, Md.

Luo, C., N. Mahowald, and J. del Corral (2003), Sensitivity study of meteorological parameters on mineral aerosol mobilization, transport, and distribution, *J. Geophys. Res.*, *108*(D15), 4447, doi:10.1029/2003JD003483.

Macrellis, H., C. Trick, E. Rue, G. Smith, and K. Bruland (2001), Collection and detection of natural iron-binding ligands from seawater, *Mar. Chem.*, *76*, 175–187.

Mahowald, N., K. Kohfeld, M. Hansson, Y. Balkanski, S. Harrison, I. Prentice, M. Schulz, and H. Rodhe (1999), Dust sources and deposition during the last glacial maximum and current climate: A comparison of model results with paleodata from ice cores and marine sediments, *J. Geophys. Res.*, *104*, 15,895–15,916.

Marshall, D. (1997), Subduction of water masses in an eddying ocean, *J. Mar. Res.*, *102*, 201–222.

Marshall, J., A. Adcroft, C. Holl, L. Perelman, and C. Heisey (1997a), A finite-volume, incompressible Navier Stokes model for studies of the ocean on parallel computers, *J. Geophys. Res.*, *102*, 5753–5766.

Marshall, J., C. Hill, L. Perelman, and A. Adcroft (1997b), Hydrostatic, quasi-hydrostatic, and nonhydrostatic ocean modeling, *J. Geophys. Res.*, *102*, 5733–5752.

Martin, J. (1990), Glacial-interglacial CO_2 change: The iron hypothesis, *Paleoceanography*, *5*, 1–13.

Martin, J., G. Knauer, D. Karl, and W. Broenkow (1987), VERTEX: Carbon cycling in the northeast Pacific, *Deep Sea Res., Part A*, *34*, 267–285.

Martin, J., et al. (1994), Testing the iron hypothesis in ecosystems of the equatorial Pacific Ocean, *Nature*, *371*, 123–129.

McKinley, G., M. Follows, and J. Marshall (2004), Mechanisms of air-sea CO_2 flux variability in the equatorial Pacific and the North Atlantic, *Global Biogeochem. Cycles*, *18*, GB2011, doi:10.1029/2003GB002179.

Mitchell, B., E. Brody, O. Holm-Hansen, C. McClain, and J. Bishop (1991), Light

limitation of phytoplankton biomass and macronutrient utilization in the Southern Ocean, *Limnol. Oceanogr.*, *36*, 1662–1677.

Parekh, P., M. Follows, and E. Boyle (2004), Modeling the global ocean iron cycle, *Global Biogeochem. Cycles*, *18*, GB1002, doi:10.1029/2003GB002061.

Parekh, P., M. Follows, and E. Boyle (2005), Decoupling of iron and phosphate in the global ocean, *Global Biogeochem. Cycles*, GB2020, doi:10.1029/2004GB002280.

Parekh, P., S. Dutkiewicz, M. Follows, and T. Ito (2006), Atmospheric carbon dioxide in a less dusty world, *Geophys. Res. Lett.*, *33*, L03610, doi:10.1029/2005GL025098.

Petit, J., et al. (1999), Climate and atmospheric history of the past 420,000 years from the Vostok ice core, Antarctica, *Nature*, *399*, 429–436.

Popova, E., V. Ryabchenko, and M. Fasham (2000), Biological pump and vertical mixing in the Southern Ocean: Their impact on atmospheric CO_2, *Global Biogeochem. Cycles*, *14*, 477–498.

Rea, D. (1994), The paleoclimatic record provided by eolian deposition in the deep sea: The geologic history of wind, *Rev. Geophys.*, *32*, 159–195.

Rea, D., J. Zachos, and R. Owen (1990), Global change at the Paleocene-Eocene boundary—Climatic and evolutionary consequences of tectonic events, *Palaeogeor. Palaeoclimatol. Palaeoecol.*, *79*, 117–128.

Redfield, A. (1958), The biological control of chemical factors in the environment, *Am. Sci.*, *46*, 205–221.

Rue, E., and K. Bruland (1995), Complexation of iron (III) by natural organic ligands in the central North Pacific as determined by a new competitive ligand equilibration/adsorptive cathodic stripping voltammetric method, *Mar. Chem.*, *50*, 117–138.

Rue, E., and K. Bruland (1997), The role of organic complexation on ambient iron chemistry in the equatorial Pacific Ocean and the response of a mesoscale iron addition experiment, *Limnol. Oceanogr.*, *42*, 901–910.

Sarmiento, J., N. Gruber, M. A. Brzezinski, and J. P. Dunne (2004), High-latitude controls of thermocline nutrients and low latitude biological productivity, *Nature*, *427*, 56–60.

Sigman, D., D. McCorkle, and W. Martin (1998), The calcite lysocline as a constraint on glacial/interglacial low-latitude production changes, *Global Biogeochem. Cycles*, *12*, 409–428.

Sigman, D. M., and E. A. Boyle (2000), Glacial/interglacial variations in atmospheric carbon dioxide, *Nature*, *407*, 859–869.

Stephens, B., and R. Keeling (2000), The influence of Antarctic sea ice on glacial-interglacial CO_2 variations, *Nature*, *404*, 171–174.

Toggweiler, J. (1999), Variation of atmospheric CO_2 by ventilation of the ocean's deepest water, *Paleoceanography*, *14*, 571–588.

Toggweiler, J., and B. Samuels (1998), On the ocean's large-scale circulation near the limit of no vertical mixing, *J. Phys. Oceanogr.*, *28*, 1832–1852.

Trenberth, K., J. Olson, and W. Large (1989), A global ocean wind stress climatology based on ECMWF analyses, *Tech. Rep. NCAR/TN-338+STR*, Natl. Cent. for Atmos. Res., Boulder, Colo.

Tsuda, A., et al. (2003), A mesoscale iron enrichment in the western subarctic Pacific induces a large centric diatom bloom, *Science*, *300*, 958–961.

van Oijen, T., M. van Leeuwe, E. Granum, F. Weissing, R. Bellerby, W. Gieskes, and H. de Baar (2004), Light rather than iron controls photosythate production and allocation in Southern Ocean phytoplankton populations during austral autumn, *J. Plankton Res.*, *26*, 885–900.

Walin, G. (1982), On the relation between sea-surface heat flow and thermal circulation in the ocean, *Tellus*, *34*, 187–195.

Wanninkhof, R. (1992), Relationship between wind-speed and gas-exchange over the ocean, *J. Geophys. Res.*, *97*, 7373–7382.

Watson, A., D. Bakker, A. Ridgwell, P. Boyd, and C. Law (2000), Effect of iron supply on Southern Ocean CO_2 uptake and implications for glacial atmospheric CO_2, *Nature*, *407*, 730–733.

Wells, M., N. Price, and K. Bruland (1995), Iron chemistry in seawater and its relationship to phytoplankton: A workshop report, *Mar. Chem.*, *48*, 157–182.

Williams, R., and M. Follows (1998), The Ekman transfer of nutrients and maintenance of new production over the North Atlantic, *Deep Sea Res., Part I*, *45*, 461–489.

Witter, A., D. Hitchins, A. Butler, and G. Luther (2000), Determination of conditional stability constants and kinetic constants for strong model Fe-binding ligands in seawater, *Mar. Chem.*, *69*, 1–17.

Wu, J., E. Boyle, W. Sunda, and L. Wen (2001), Soluble and colloidal iron in the oligotrophic North Atlantic and North Pacific, *Science*, *293*, 847–849.

Yamanaka, Y., and E. Tajika (1997), Role of dissolved organic matter in the marine biogeochemical cycles: Studies using an ocean biogeochemical general circulation model, *Global Biogeochem. Cycles*, *11*, 599–612.

S. Dutkiewicz and M. J. Follows, Department of Earth, Atmosphere and Planetary Science, Massachusetts Institute of Technology, Cambridge, MA 02139, USA.

T. Ito, Joint Institute for the Study of Atmosphere and Ocean, University of Washington, Seattle, WA 98195-4235, USA.

P. Parekh, Climate and Environmental Physics, Physics Institute, Sidlerstrasse 5, 3012 Bern, Switzerland. (parekh@climate.unibe.ch)